Journal of Applied Polymer Science

Investigation on High Strength Laser Welds of Polypropylene and High-Density Polyethylene

Thomas Brokholm Juhl, Jesper deClaville Christiansen, Erik Appel Jensen
Department of Mechanical and Manufacturing Engineering at Aalborg University, Fibigerstraede 16, 9220 Aalborg Ø, Denmark
Correspondence to: T. B. Juhl (E-mail: thjuhl@m-tech.aau.dk)

ABSTRACT: Mechanical strength in polymer weld interfaces in semi-crystalline high density polyethylene (HDPE) and polypropylene (PP) is investigated. The welding method investigated is through transmission laser welding (TTLW). Utilizing the TTLW process with 0.4 wt % carbon black as absorber, a lap-joint is formed which is tested for mechanical properties using an Instron tensile testing machine. In contrast to earlier investigations, the tensile tests conclude that 89% of the strength of a HDPE/HDPE weld was developed in a PP/HDPE weld with HDPE as the absorbing part. This high weld strength is explained from: (1) a relatively low reptation time being in the millisecond range for both HDPE and PP; (2) a polymer mesh size (tube diameter (a)) being similar to the equilibrium interpenetration depth, determined from Helfand's theory and the interaction parameter (χ); (3) The selected HDPE and PP were both metallocene catalyzed and constituted a similar crystallization temperature which is required for high crystallinity in/near the interface. © 2013 Wiley Periodicals, Inc. J. Appl. Polym. Sci. 129: 2679–2685, 2013

KEYWORDS: polyolefins; rheology; differential scanning calorimetry (DSC); surfaces and interfaces

Received 20 November 2012; accepted 5 January 2013; published online 30 January 2013
DOI: 10.1002/app.39000

INTRODUCTION

Polymer weld interfaces are ubiquitous. Welded joints appear in plastic products,[1,2] polymer weld interfaces, and in polymeric paints. In polymeric paints solvent evaporates and polymer particles coalesce and interdiffuse a radius of gyration.[3,4] Welds also appear in polymer blends, e.g., PE/PP blends[5,6] or in rubber toughened polymers, such as nylons, PS, or epoxies.[7] Moreover, the mechanisms behind self-healing materials are comparable to weld interface formations,[8,9] and finally controllability of nanomaterials in the development of stimuli responsive materials also known as smart materials are also of interest. Stimuli could be mechanical or optical.[10,11]

Welding of dissimilar materials has been investigated for various processes, especially hot processes.[12–15] More specifically, hot tool welding of PP and PE has also been carried out with success, i.e., achievement of high-strength welds.[5,16]

Usually PP and PE are considered weld incompatible,[12,17,18] but Chaffin et al.[5] were able to weld the two by selecting metallocene catalyzed PE and PP. Metallocene catalysis secures a narrower molecular weight distribution and high or certain isotacticity, leading to improved crystallinity at the polymer surface. Zhang et al.[16] succeeded by selecting an impact propylene copolymer, which is a polypropylene co-polymerized with an ethylene rubber phase, ensuring compatibility to the PE in the weld interface.

Both weld interfaces were prepared using a heated tool methodology with weld times of 20 min[5] and 15 min,[16] which is slow from an industrial point of view. For industrial welding new technologies have been emerging, such as laser welding, which have drawn a lot of attention over the last decade due to its relatively low cost, flexibility, and high quality.[19]

The specific process of interest here is the through transmission laser welding (TTLW) process, which is presented in Figure 1. The basic idea is that a part transparent to the incident laser wavelength is placed on top of a part absorbing the wavelength (usually because of light absorbing particles added to the polymer)—resulting in a so-called lap-joint. The laser beam will heat up and melt the absorbing part which will wet, heat up, and melt the transparent part. When both materials are molten and wetting has occurred, the polymer molecules are able to inter-diffuse and form entanglements. What is often varied in the process is laser power and weld speed.[19]

Literature and theoretical studies concerning weld line formation often focus on reptation mechanisms in the weld interface.[5,12–14] The models are theoretical and predict interpenetration as a function of time. However, the magnitude of the reptation time is rarely reported.

Therefore, the scope of this article is to evaluate reptation time and compare it with the time in molten state, which for laser

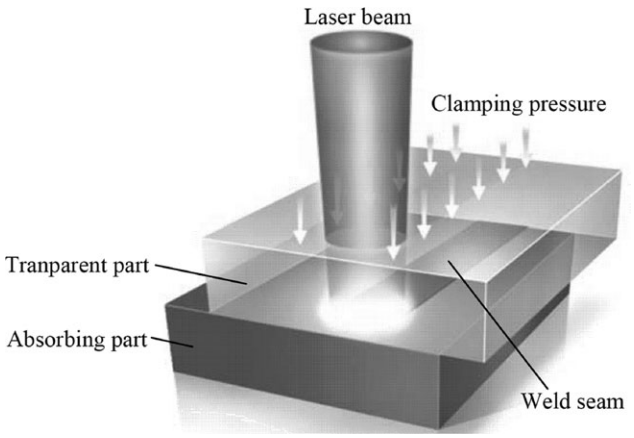

Figure 1. Sketch of the laser weld. (Reproduced from Ref. 20, with permission from LPKF Laser and Electronics AG.)

welding is reported to be in the range of seconds.[21] If the reptation time is much shorter than the process time, strong laser welds are feasible. It will also be investigated whether metallocene catalyzed HDPE and PP are weldable with lasers or not.

THEORY

Reptation Models

One way to quantify the diffusion of polymers at the interface is using reptation models. The concept of reptation is to model the polymer melt entanglements as a chain constricted by a surrounding tube. The chain can then move back and forth within the tube and can only escape at the tube ends. The time it takes to escape the tube is defined as reptation time, and therefore during reptation time a polymer chain has diffused one radius of gyration, R_g.[12]

The reptation model dates back to de Gennes,[22] who was the first to propose polymer dynamics caused by reptation mechanisms. Later Doi and Edwards[23] expanded the model, making it possible to link the macroscopic zero shear viscosity, η_0, to the microscopic reptation time, τ_{rep}, for an entangled linear polymer melt through:[24]

$$\eta_0 = \frac{\pi^2 c k_B T}{20 N_e} \tau_{rep} \tag{1}$$

where c is the number density of monomers, and therefore equals $\rho N_A/M_0$, where ρ is the melt density and M_0 is the monomer molecular weight. To determine the reptation time, it is also noticeable that it depends linearly on η_0, which varies with temperature. Therefore eq. (1) can be rewritten to:

$$\tau_{rep}(T) = \frac{20 N_e M_0}{\pi^2 k_B T \rho N_A} \eta_0(T) = \frac{20 M_e}{\pi^2 R T \rho} \eta_0(T), \tag{2}$$

where M_e ($=N_e\ M_0$) is the molecular weight between entanglements, N_e is the number of monomers between entanglements, $R = k_B N_A$ is the gas constant, $\rho(T)$ is the temperature dependent melt density.

Moreover, the reptation model also reveals following result for the reptation time:[24]

$$\tau_{rep}(T) = \frac{\zeta(T) N_K{}^3 b_K{}^4}{\pi^2 k_B T a^2}, \tag{3}$$

where N_K is the number of monomers, b_K is the Kuhn monomer length (also known as a statistical segment length), k_B is Boltzmann's constant, a is the tube diameter, and $\zeta(T)$ is the temperature dependent monomeric friction coefficient. According to the Volger-Fulcher equation the temperature dependence of ζ is as:[25]

$$\ln \zeta(T) = A + \frac{B}{T - C}, \tag{4}$$

where A, B, and C are constants. It is important to note that the reptation model and the Vogel-Fulcher equation are suggested independently of each other. Likewise, they are based on approximations and are therefore not fundamental laws of physics.[25]

Polymer Miscibility

An important criterion for mutual diffusion of polymers is polymer-polymer miscibility, i.e., the ability of two polymers to mix and be in one phase at thermodynamic equilibrium. This can be estimated using the Flory-Huggins (FH) theory for polymer-polymer mixtures.[12,26,27] The FH theory states that mixing occurs if the Gibbs free energy (ΔG) is reduced, i.e., $\Delta G = \Delta H - T{\cdot}\Delta S < 0$. ΔH (enthalpy) of mixing is positive when mixing two polymers, while ΔS (entropy) of mixing is negative. When mixing two polymers, the entropic gain is very low (close to zero) due to combinatorial restrictions. Therefore, ΔH becomes predominant and $\Delta G > 0$, i.e., phase separation. Specifically, it is shown that two polymers with a high molecular weight ($M_w \sim 10^5$ g/mol) are immiscible, even though their solubility parameters (δ) are only slightly different.[28]

Helfand's Theory

Based on the FH theory, commercial polymers consisting of dissimilar polymers, such as PP and HDPE, should be immiscible—and therefore not weldable. However, thermodynamically immiscible polymers like PP and HDPE have been shown to be weldable,[5] and one explanation can be obtained from Helfand's theory, which correlates the equilibrium interfacial width (w_∞) with the FH interaction parameter (χ).[13,29] The equilibrium interfacial width is the interpenetration depth achieved when the polymers are at thermodynamical equilibrium. χ can be expressed through differences in solubility parameter as:[30]

$$\chi = \frac{V_m(\delta_1 - \delta_2)^2}{RT} \tag{5}$$

where V_m is the molar volume, which in this case is the average molar volume of the two polymers. The temperature of interest for semicrystalline polymers is the crystallization temperature, since this defines temperature at which the chains are "frozen in."[31] Helfand's equation is:[14]

$$w_\infty = 2\sqrt{\frac{b_1 + b_2}{12 \cdot \chi}} \tag{6}$$

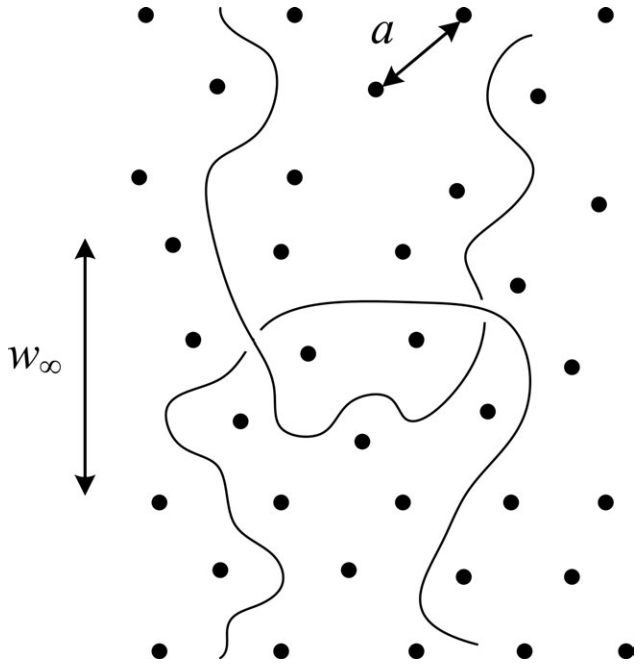

Figure 2. Illustration of the mesh size mesh size. This is a two polymer system; therefore, two mesh sizes. Note the possibility of entanglement formation when w_∞ is comparable to a.

where b_i is the statistical segment length of segment i. The infinity symbol refers to the molecular weight which is approaching infinity. For commercial plastics this assumption is very good.[13]

Entanglement Spacing

For strength development at the interface, not only the interfacial width is important, also the entanglement mesh size of the entangled polymer network plays a role. If the mesh size is large, the polymer interface also needs a large w_∞ to ensure entanglements. On the other hand, a small w_∞ may be enough if the network mesh size is small in comparison. A typical measure of the mesh size is the tube diameter, a.[24] All this is illustrated in Figure 2 for a system where $w_\infty > a$.

EXPERIMENTAL

Materials

For the investigation a metallocene catalyzed high-density polyethylene homopolymer (mHDPE) from Total Petrochemicals and a metallocene catalyzed polypropylene homopolymer (mPP) from LyondellBasell were selected, see Tables I and II for more information. Note that the tacticity of the PP is tailored from the supplier to constitute some isotactic and some atactic regions. As absorber in the laser weld an ENSACO 260 G carbon black from Timcal was utilized.

Table I. Material Data

Material	Commercial name	M_n [g/mol]	M_w [g/mol]	PDI	T_{melt} [°C]
mHDPE	mPE M 6091	55,100	128,000	2.3	133
mPP	Metocene HM 562 S	107,000	237,000	2.2	145

Sample Preparation for Laser Welding

The absorbing material for laser welding was 0.40 wt % carbon black, which was melt blended into the polymer matrix in a twin screw extruder setup. The setup was from Thermo Scientific, Waltham, Massachusetts, which consisted of a PRISM Eurolab 16 TSE equipment with an automatic granule feeder, six temperature-controlled barrel zones, a stainless steel water bath and an L-002-1345 pelletizer, see Ref. 34 for further description. The melt blending was performed twice to secure optimum dispersion. The process specifications are given in Table III.

All four materials (i.e., mPP and mHDPE, both with and without carbon black) were injection molded into square pieces of 110 × 110 × 1.0 mm with a film inlet in an Engel HS 1300-650 injection molding machine. Afterwards, the plates were divided into four squares measuring 55 × 55 × 1.0 mm. Process specifications are given in Table III. In the following the CB containing materials have the prefix "a" (for absorbing) and the pure materials have a prefix "t" (for transparent).

Laser Welding Experiments

The transparent piece was placed on top of the absorbing piece as illustrated in Figure 1 and clamped together under 4 bar pressure in a laser welding cell. The laser used was a diode laser, Laserline 300 W, with a wavelength of 808 nm equipped with an Arges scanner. The laser intensity was fixed to 50 W, while the weld speed was varied. The welding processes were performed 24 h or more after molding.

Mechanical Testing of Weld Specimens

Mechanical testing was inspired by DIN EN 14869-2.[35] The cut out weld specimens indicated with dashed lines in Figure 3 were tensile tested in an Instron 5944 tensile testing machine equipped with a 2 kN load cell. For all tests the grips were located 63 mm apart and the tests were performed with a speed of 50 mm/min. The test was a shear stress test and the reported strength was the force required to fracture the test specimen

Table II. Polymer Physics Data

Symbol	Description	mHDPE	mPP
b [Å][a]	Statistical segment length	5.64	5.25
b_K [nm][b]	Kuhn segment length	1.37	1.14
a [nm][b]	Tube diameter	3.60	6.90
M_e [g/mol][b]	Molecular weight between entanglements	832	3880
M_0 [g/mol][b]	Monomer molar mass	28.06	42.08
ρ_{melt} [kg/m^3][c]	Melt density	785	766
δ [MPa$^{1/2}$][c]	Solubility parameter	16.0	17.0
V_m [cm^3/mol][c]	Molar volume	32.9	49.1
ΔH_m^0 [J/g][c]	Spec. heat of melting	285	207

[a]Ref. 12.
[b]Ref. 32.
[c]Ref. 33.

Table III. Process Parameters for Melt Blending and Injection Molding

	mHDPE	mPP
Extruding temp. [°C]	180	180
Screw speed [rpm]	200	200
Feed rate [kg/h]	~2.5	~2.5
Inj. Molding melt temp [°C]	200	220
Tool temp. [°C]	50	50
Cooling time [s]	40	30
Cycle time [s]	48.3	38.3
Injection speed [mm/s]	25	25

divided by the weld specimen length, which was approximately 10 mm; the exact length was measured with a slide gauge for each specimen. Five repetitions were used for each sample.

Rheometry

As indicated in Reptation Models the main purpose using rheometry was to determine η_0 as function of temperature, which was used to determine the reptation time as function of temperature as presented in eq. (2).

The zero shear viscosity is determined with a Paar Physica MCR500 rheometer in a plate-plate configuration with a 25-mm disc and a gap height of 1 mm. In order to measure within the linear elastic regime, the oscillatory tests were performed with small strain amplitude, $\gamma = 0.05$. The angular frequency varied from 0.0628 to 628 rad/s. η_0 was determined as the viscosity at 0.0628 rad/s. The two polymers both have a narrow molecular weight distribution and are linear; thus, the Cox-Merz rule is assumed valid and applied.[36]

Each specimen was melted for 5 min, the required gap height was established, and the specimen was equilibrated for another 5 min before measurement. The test material was taken from granules (ca. 0.5 g), and no repetitions were performed.

Differential Scanning Calorimetry (DSC)

Thermal characterization of the materials was done by DSC using a Q2000 from TA Instruments. Materials were cut out from the injection molded plates using a punch plier (ca. 15 mg of material). The materials were placed in aluminum pans according to TA Instrument's Tzero series. All samples were equilibrated at 20°C and heated/cooled at a rate of 10 K/min to 200°C for mHDPE and 220°C for mPP. The test was performed with N_2 as a purge gas with a flow rate of 50 mL/min. Three heating/cooling cycles are used.

The parameters of interest from DSC measurement are: (1) T_m, defined as the temperature at the endothermic peak observed during heating; (2) T_c, defined as the temperature at the exothermic peak observed during cooling; (3) degree of crystallinity (α_c), defined by:

$$\alpha_c = \frac{\Delta H_m}{\Delta H_m{}^0} \cdot 100\% \quad (7)$$

where ΔH_m is the heat of fusion given as the area between the endothermic peak during heating and the baseline. $\Delta H_m{}^0$ is listed in Table II. For determination of crystallinity only the first up-scan is used.

RESULTS AND DISCUSSION

Mechanical Testing of Laser Welds

The weld specimens are tensile tested, and their strength are determined according to the method described in Laser Welding Experiments. The strength is then plotted as function of the process line energy, which is defined as the laser power divided by laser speed. The final plot is presented in Figure 4. The smooth lines in the figure are shape preserving interpolants to highlight the trends.

As seen in the figure, all four combinations seem to reach an optimum strength, i.e., too low line energy is not enough for melting the interface and too high line energy decomposes the material. Note that the weld strength optimum for aPP/tPP is achieved at a lower line energy than aHDPE/tHDPE. This can be explained with PP being more transparent than HDPE

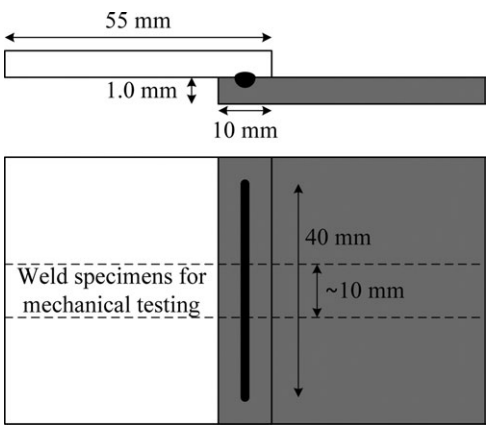

Figure 3. Illustration of the weld specimen and the cut out specimen for mechanical testing.

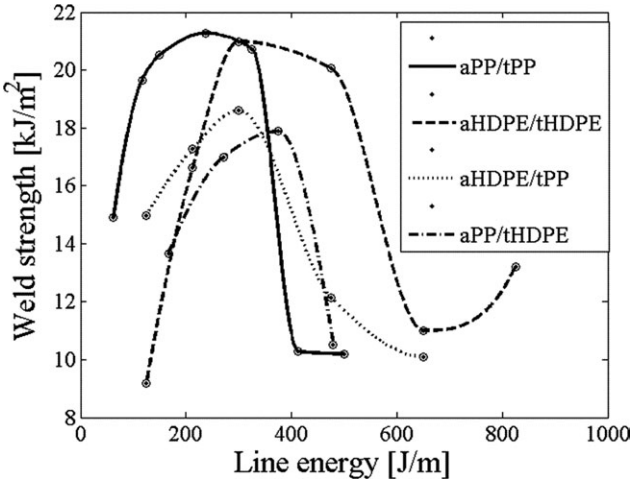

Figure 4. Weld strength versus line energy for the four combinations of PP and HDPE.

Table IV. The Maximum Weld Strength from Figure 4 and the Corresponding Line Energy and Weld Speed

Best weld	aPP/tPP	aHDPE/tHDPE	aHDPE/tPP	aPP/tHDPE
Weld strength [kJ/m^2]	21.3 ± 4.5	21.0 ± 1.0	18.6 ± 1.7	17.9 ± 1.4
Laser speed [mm/s]	210.5	166.7	166.7	133.3
Line energy [J/m]	237.5	299.9	299.9	375.1
Laser power [W]	50.0	50.0	50.0	50.0

(probably due to higher crystallinity, see Differential scanning calorimetry (DSC)).

Table IV seems to conclude that aHDPE/tPP is more weldable compared with aPP/tHDPE. This can also be explained from the greater transparency of PP. Moreover, if the standard deviations are taken into account, aHDPE/tPP and aPP/tHDPE are able to achieve the same strength. By comparing their strength to the weakest of the parent materials (aHDPE/tHDPE), the strength has developed 18.7/21.0 = 89%. Thus, the polymers are to some degree weldable, even though the opposite is often reported.

Rheometry

The reptation time of the selected mPP and mHDPE are determined from the zero shear viscocity (η_0). A frequency sweep is performed on the two polymers as presented in Figures 5 and 6.

When η_0 is known at different temperatures, the reptation time (τ_{rep}) and monomeric friction coefficient (ζ) can be found from eqs. (2) and (3), respectively. By calculation, ζ can be determined at various temperatures as plotted in Figures 7 and 8.

As a comparison to literature the monomeric friction coefficient is reported to; $\zeta_{HDPE}(190°C) = 4.74 \cdot 10^{-13}$ kg/s,[37] $\zeta_{HDPE}(190°C) = 1.30 \cdot 10^{-12}$ kg/s,[38] $\zeta_{iPP}(190°C) = 1.04 \cdot 10^{-12}$ kg/s,[37] $\zeta_{iPP}(190°C) = 1.86 \cdot 10^{-12}$ kg/s.[37] The difference for iPP is explained by differences in M_e. Using the Volger-Fulcher equation, the fitted model predicts: $\zeta_{mHDPE}(190°C) = 3.40 \cdot 10^{-13}$ kg/s and $\zeta_{mPP}(190°C) = 1.60 \cdot 10^{-12}$ kg/s. Thus, the fitted model is near the values reported in literature.

From knowledge of the ζ values, the reptation times can be calculated. The relationship between reptation time and temperature is shown in Figure 9.

As seen from Figure 9, the reptation time for mPP and mHDPE is within the range of milliseconds; thus, the reptation mechanism cannot be the limiting factor for weld strength establishment in welding of these polymers; other mechanisms must therefore be dominating for strength establishments. In addition to this, experiments have been performed at temperatures just above the glass transition temperature leading to long reptation times, which resulted in only partial strength development.[12,39]

Differential Scanning Calorimetry (DSC)

DSC was performed to evaluate the melting and crystallization temperature of mPP and mHDPE. Also the degree of crystallinity of the injection molded plates was determined. The results are presented in Table V.

The thermal properties for mHDPE and mPP are slightly changed by addition of 0.4 wt % carbon black; the crystallization temperature is slightly increased, meaning that the CB particles have nucleating effects on the polymer matrix.

mHDPE and mPP, which from mechanical testing was concluded weldable, constitute a similar crystallization temperature; the difference is within 2°C. This similarity might be the

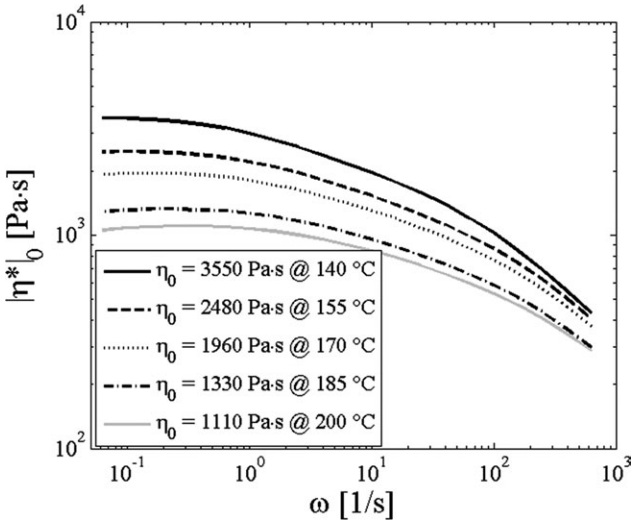

Figure 5. Frequency sweep of the mHDPE grade at various temperatures.

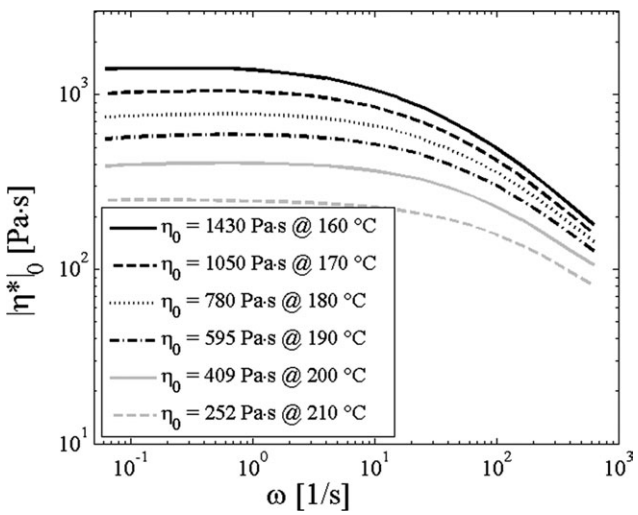

Figure 6. Frequency sweep of the mPP grade at various temperatures.

Applied Polymer SCIENCE

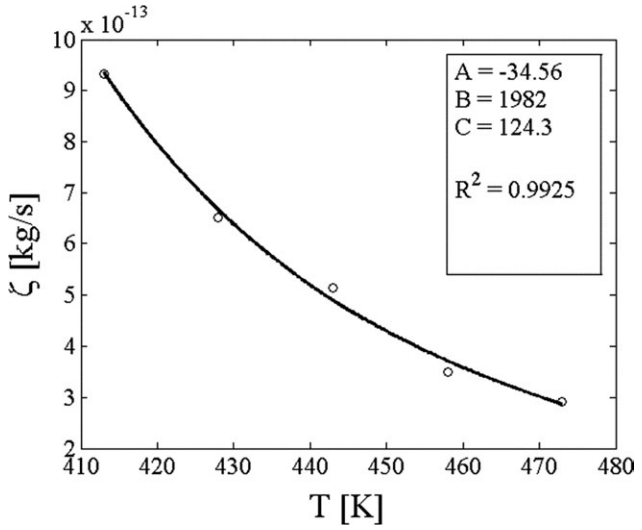

Figure 7. Monomeric friction coefficient versus temperature for mHDPE. The data points are calculated values of ζ, while the line is a fit of the Volger-Fulcher equation from eq. (4).

explanation for weld compatibility, since the entanglements are frozen in simultaneously. This simultaneous crystallization can also explain the maximum strength at a certain line energy; the optimum line energy is where the polymer are molten enough to achieve intimate contact, but also a few spheruslites are retained, which can be used as nucleation initiators during crystallization. This results in a crystalline interface, and not just amorphous, leading to enhanced strength.[31] Moreover, the greater transparency of mPP can be explained from the lower degree of crystallinity.

Predictions from Helfand's Theory

For utilization Helfand's theory from eq. (6), the Flory-Huggins interaction parameter (χ) is essential to determine. Simply, eq. (5) gives:

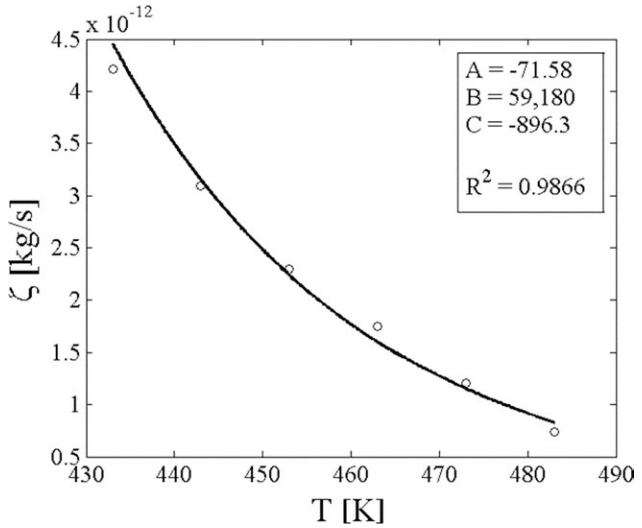

Figure 8. Monomeric friction coefficient versus temperature for mHDPE. The data points are calculated values of ζ, while the line is a fit of the Volger-Fulcher equation from eq. (4).

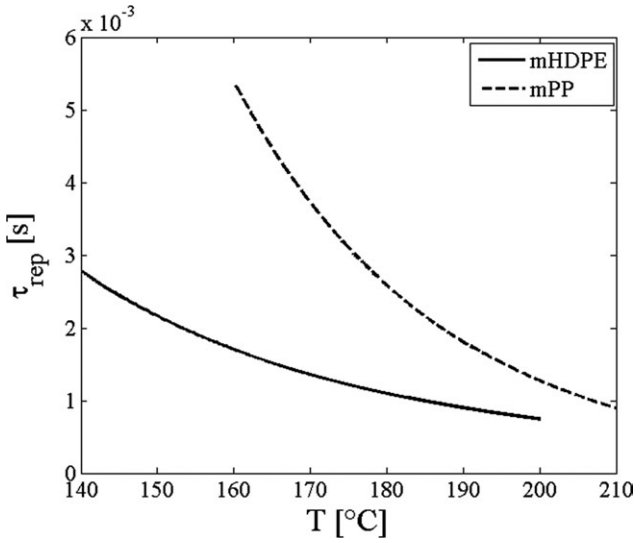

Figure 9. The reptation time of the selected mHDPE and mPP versus temperature.

$$\chi = \frac{2(32.9\,\frac{\mathrm{cm}^2}{\mathrm{mol}} + 49.1\frac{\mathrm{cm}^2}{\mathrm{mol}})(17.0\sqrt{\mathrm{MPa}} - 16.0\sqrt{\mathrm{MPa}})^2}{8.314\,\frac{\mathrm{J}}{\mathrm{mol\cdot K}}\cdot(120.4\mathrm{K} + 273.15\mathrm{K})} = 0.0125 \tag{8}$$

This can be compared to the χ parameter from Jeon et al.,[40] who have estimated the value between a head-to-head PP and HDPE using SANS, giving $\chi = -0.0311 + 17.60/T$. Using a temperature of 120.4°C (393.3 K), $\chi = 0.0137$.

From eq. (6), the equilibrium inter-penetration depth can be predicted to:

$$w_\infty = 2\sqrt{\frac{(5.25\text{Å})^2+(5.64\text{Å})^2}{12\cdot 0.0125}} = 39.8\text{Å} \tag{9}$$

Using the χ value from Ref. [40], w_∞ can be calculated to 38.0 Å. These approximately 4 nm is also reported in literature.[5]

An equilibrium inter-penetration depth of approximately 4 nm is comparable to the tube diameter of 3.6 and 6.9 nm of HDPE and PP, respectively. Therefore, interfacial entanglements are possible, and mechanical strength can be developed.

CONCLUSIONS

Weldability between two selected HDPE and PP, both of metallocene catalysis, was investigated using through transmission laser welding (TTLW). First of all the reptation time of the two

Table V. Results from DSC of mHDPE and mPP with and Without Carbon Black

Material	tHDPE	aHDPE	tPP	aPP
T_m [°C]	132.4	132.5	147.4	146.9
T_c [°C]	119.2	120.4	118.3	119.3
ΔH_m [J/g]	163.0	164.7	71.83	73.07
α_c [%]	57.2	57.8	34.7	35.3

was determined to be within the millisecond range, e.g., at 170°C the reptation time was estimated to 1.36 ms and 3.72 ms for HDPE and PP, respectively. Since the reptation time is orders of magnitude shorter than the time in molten phase, it is to conclude that time is not a limiting factor when laser welding at relatively high temperatures.

Moreover, it was found out that the selected HDPE and PP was weldable with 89% of the strength of a HDPE/HDPE weld. This was explained from the interaction parameter and Helfand's theory, which was compared to the tube diameter (a) of HDPE and PP. From this it is to conclude that the two polymers interdiffuse 4.0 nm into each other, which is comparable to the tube diameters of 3.6 nm and 6.9 nm; thus, entanglements can form. In other words, a suggested welding criterion is; $w_\infty > a$. Some of the strength establishment might also be caused by mechanical interlocking, which has not been investigated.

Additionally, this model and method might be harnessed to as a tool for predicting polymer weldability in general.

ACKNOWLEDGMENTS

Financial support by the Danish Strategic Research Council through project "Expanding the Weld Compatibility of Plastics" is gratefully acknowledged, and thanks to Coloplast for usage of their laser welding facilities.

REFERENCES

1. Rotheiser, J. Joining of Plastics—Handbook for Designers and Engineers, 3rd ed.; Hanser, Munich, Germany, **2009**.
2. Staff, P. Handbook of Plastics Joining—A Practical Guide; William Andrew, Norwich, NY, USA, **1998**.
3. Wool, R. P. Fundamentals of Fracture in Bio-Based Polymers; Elsevier—Academic Press, Munich, Germany, **2005**.
4. Jones, R. A.L.; Richards, R. W. Polymers at Surfaces and Interfaces; Cambridge University Press, Stoneham, MA, USA, **1999**.
5. Chaffin, K.A.; Knutsen, J. S.; Brant, P.; Bates, F. S. *Science* **2000**, *288*, 2187.
6. Shanks, R. A.; Li, J.; Yu, L. *Polymer* **2000**, *41*, 2133.
7. Swallowe, G. M. Mechanical Properties and Testing of Polymers—An A-Z Reference; Dordrecht: Kluwer Academic, **1999**.
8. Wool, R. P. *Nature* **2001**, *409*, 773.
9. Wool, R. P. *Soft Matter* **2008**, *4*, 400.
10. Ariga, K.; Mori, T.; Hill, J. P. *Adv. Mater.* **2012**, *24*, 158.
11. Boyle, M. M.; Smaldone, R. A.; Whalley, A. C.; Ambrogio, M. W.; Botros, Y. Y.; Stoddart, J. F.. *Chem. Sci.* **2011**, *2*, 204.
12. Wool, R. P. Polymer Interfaces—Structure and Strength; Munich: Hanser Publishers, **1995**.
13. Lo, C. T.; Narasimhan, B. *Polymer* **2005**, *46*, 2266.
14. Cole, P.; Cook, R.; Macosko, C. *Macromolecules* **2003**, *36*, 2808.
15. Yang, L.; Suo, T.; Niu, Y.; Wang, Z.; Yan, D.; Wang, H. *Polymer* **2010**, *51*, 5276.
16. Zhang, C.; Chen, R.; Chen, F.; Shangguan, Y.; Zheng, Q.; Hu, G. *Chin. J. Polym. Sci.* **2011**, *29*, 497.
17. Kammer, H. W. *Polym. Networks Blends* **1995**, *5*, 69.
18. Teh, J. W.; Rudin, A.; Keung, J. C. *Adv Polym. Technol.* **1994**, *13*, 1.
19. Klein, J. *Science* **1990**, *250*, 640.
20. LPKF Laser and Electronics AG, Laser Plastic Welding—Innovative Joining Technology for the Electronics Industry, Erlangen, Germany; **2012**. Available at: http://www.lpkf.com/_images/1834-laser-welding.jpg.
21. Mayboudi, L. S.; Birk, A. M.; Zak, G.; Bates, P. J. *J. Laser Appl.* **2010**, *22*, 22.
22. Gennes, P. G. D. *J. Chem. Phys.* **1971**, *55*, 572.
23. Doi, M.; Edwards, S. F. The Theory of Polymer Dynamics; Oxford, GB: Oxford University Press, **1986**.
24. Doi, M. Introduction to Polymer Physics; Oxford: Clarendon Press, **1996**.
25. Dealy, J. M.; Larson, R. G. Structure and Rheology of Molten Polymers—From Structure to Flow Behavior and Back Again; Munich, Germany: Hanser, **2006**.
26. Bower, D. I. An Introduction to Polymer Physics; Cambridge: Cambridge University Press, **2002**.
27. Flory, P. J. *J. Chem. Phys.* **1942**, *10*, 51.
28. Oh, S. Y.; Bae, Y. C. *Eur. Polym. J.* **2010**, *46*, 1328.
29. Helfand, E.; Sapse, A. M. *J Chem Phys* **1975**, *62*, 1327.
30. Hiemenz, P. C.; Lodge, T. P. Polymer Chemistry, 2nd ed.; New York, NY, USA: CRC Press, **2007**.
31. Godail, L.; Packham, D. *J. Adhes. Sci. Technol.* **2001**, *15*, 1285.
32. Fetters, L. J.; Lohse, D. J.; Colby, R. H. Chain Dimensions and Entanglement Spacings; Springer: New York, **2007**.
33. Krevelen, D. W. V.; Nijenhuis, K. T. Properties of Polymers, 4th ed.; Amsterdam, Netherlands: Elsevier, **2009**.
34. Klitkou, R.; Jensen, E. A.; Christiansen, J. D. C. *J. Appl. Polym. Sci.* **2012**, *126*, 620.
35. Jaeschke, P.; Herzog, D.; Haferkamp, H.; Peters, C.; Herrmann, A. S. *J. Reinf. Plast. Compos.* **2010**, *29*, 3083.
36. Wen, Y. H.; Lin, H. C.; Li, C. H.; Hua, C. C. *Polymer* **2004**, *45*, 8551.
37. Meerveld, J. V. *Rheol. Acta* **2004**, *43*, 615.
38. Vega, J. F.; Rastogi, S.; Peters, G. W. M.; Meijer, H. E. H. *J. Rheol.* **2004**, *46*, 663.
39. Boiko, Y. M.; Bach, A.; Lyngaae-Jørgensen, J. *J. Polym. Sci. Part B: Polym. Phys.* **2004**, *42*, 1861.
40. Jeon, H.; Lee, J.; Balsara, N. *Macromolecules* **1998**, *31*, 3328.